Effects of Composition and Annealing on the Electrical Properties of $CoSb_3$

Arwyn L. E. Smalley, Seok Kim, and David C. Johnson*

Chemistry Department, 1253 University of Oregon, Eugene, Oregon 97403

Received April 1, 2003. Revised Manuscript Received July 10, 2003

A series of $CoSb_3$ samples was synthesized at low temperature (∼150 °C) using modulated elemental reactants, with composition varying between Co-rich and Sb-rich, resulting in lattice parameters ranging from 9.023 to 9.090 Å. The samples were annealed in 100 °C increments from 200 to 600 °C, with lattice parameter, electrical resistivity, and Seebeck coefficient measured after each annealing. The spread of lattice parameters decreased with annealing (9.045 to 9.062 Å). The electrical resistivity of the samples changed from being nominally temperature independent, characteristic of a heavily doped semiconductor, to an exponential temperature dependence expected for a semiconductor, with band gaps of ∼0.1 eV. Seebeck measurements confirm the reduction in electrically active defect concentration with increasing annealing temperature. The nonequilibrium defect concentration trapped by low-temperature crystallization and varying composition, combined with the annealing studies, allowed a wide range of structural and electrical properties to manifest within a limited sample set.

I. Introduction

$CoSb_3$, with the skutterudite structure, has been studied extensively; most recently for its potential uses in thermoelectric applications. $CoSb_3$ has a cubic crystal structure, with space group $Im\bar{3}$, and is a very narrow, direct-band-gap semiconductor.[1] Single crystals, powders, and thin films of $CoSb_3$ have all been synthesized and analyzed, resulting in an extensive body of knowledge on the compound. Although the thermal conductivity of $CoSb_3$ is too high for the material to be used as a thermoelectric material, its low electrical resistivity (0.429 mΩ·cm) and relatively high Seebeck coefficient (72 μV/K) have resulted in the use of the skutterudite structure as a template for thermoelectric material design.[2] The skutterudite structure is formed of four-membered rings of the pnictide, with metal atoms octahedrally coordinated to six pnictide atoms (Figure 1). There are eight formula units per unit cell. The resulting structure resembles a cage, with a large "void", which for $CoSb_3$ is approximately 4 Å across.[3]

The lattice parameter, electrical resistivity, Seebeck coefficients, and charge carrier concentrations reported for undoped $CoSb_3$ vary considerably (see Table 1). Some of this variability seems to depend on synthetic technique, and possibly on the synthetic environment. For example, Schmidt reported two significantly different lattice sizes in samples that had been synthesized using different vapor transport gases.[3] And although undoped $CoSb_3$ is accepted to be a *p*-type semiconductor, several undoped *n*-type samples have been reported, possibly due to an Sb-poor synthetic environment.[4,5] In our own synthesis of $CoSb_3$ using modulated elemental reactants, we noted significant and reproducible differences between the lattice constants of our samples (a = 9.05 Å[6]) as compared to literature values (a = 9.034 Å[7]).

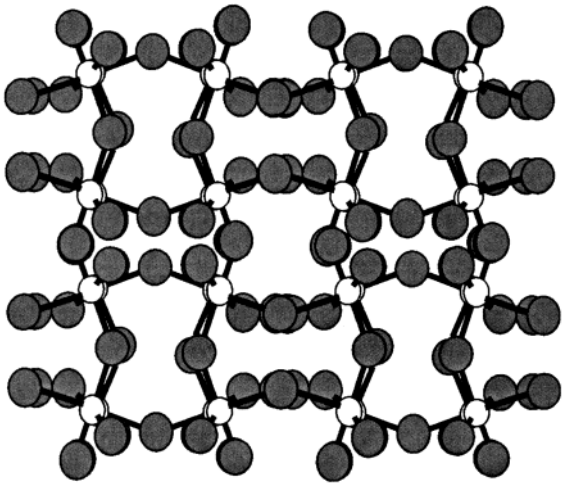

Figure 1. Cartoon of the skutterudite-type compounds. White circles indicate metal atoms and gray circles indicate pnictide atoms.

Although these syntheses of $CoSb_3$ do not intentionally include interstitial atoms or dopants, defects in the

* To whom correspondence should be addressed. Phone: 541-346-4612. Fax: 541-346-0487. E-mail: davej@oregon.uoregon.edu.

(1) Sofo, J. O.; Mahan, G. D. *Mater. Res. Symp. Proc.* **1999**, *545*, 315−320.
(2) Caillat, T.; Borshchevsky, A.; Fleurial, J.-P. *J. Appl. Phys.* **1996**, *80*, 4442−4449.
(3) Schmidt, Th.; Kliche, G.; Lutz, H. D. *Acta Crystallogr.* **1987**, *C43*, 1678−1679.
(4) Kawaharada, Y.; Kurosaki, K.; Uno, M.; Yamanaka, S. *J. Alloys Compd.* **2001**, *315*, 193−197.
(5) Sharp, J. W.; Jones, E. C.; Williams, R. K.; Martin, P. M.; Sales, B. C. *J. Appl. Phys.* **1995**, *78*, 1013−1018.
(6) Sellingschegg, H.; Smalley, A.; Yoon, G.; Johnson, D. C.; Nolas, G. S.; Kaeser, M.; Tritt, T. M. *Proc. Int. Conf. Thermoelectrics* **1999**, 18th, 352−355.
(7) Ackermann, J.; Wold, A. *J. Phys. Chem. Solids* **1977**, *38*, 1013−1016.

10.1021/cm030315o CCC: $25.00
Published on Web 08/23/2003

Table 1. Electrical and Structural Properties from a Range of Sources Illustrating the Varied Properties of CoSb3

lattice constant (Å)	electrical resistivity	Seebeck coefficient	carrier concentration	carrier type	ref.
9.0345	1.894 mΩ·cm	220 μV/K	0.116×10^{19} cm^{-3}	+	2
9.034	0.14 mΩ·cm	~1 μV/K		+	7
9.0385 or 9.0775					3
9.0369	38 mΩ·cm	310 μV/K	1.2×10^{17} cm^{-3}	+	21
	4.0 mΩ·cm	120 μV/K	5.0×10^{18} cm^{-3}	+	5
9.038 or 9.026	~2.0 mΩ·cm	~150 μV/K		− or +	4

crystal structure could change the structure sufficiently to change structural and electronic properties. Vacancies in the metal or pnictide sites, or the insertion of excess atoms in the void are expected to result in "self-doping". If there is a metal vacancy, not only would that site lack the mass and electron density from the atom, but the associated pnictide atoms would have less electron density for bonding. Similarly, if a pnictide atom was missing, the metal would have more electron density to provide to the remaining pnictogens, which could warp the lattice locally. Inserting an atom into the interstitial site results in lattice expansion as observed with ternary skutterudites. Any of these defects would also change the number of charge carriers available, affecting the electrical properties.

Although these differences are apparent in the literature, there has been no systematic investigation into the effects of these defects on the properties of $CoSb_3$. The thin film synthetic technique we use produces $CoSb_3$ samples with highly nonequilibrium defect concentrations. Because annealing is known to decrease the number of defects in a material, we can use annealing to examine how the properties change with doping concentration without needing to synthesize a large number of samples. This method is analogous to Badding's method of tuning a sample's properties using high pressure, which he uses to sweep through phase space without making a large number of samples.[8] Rather than using high pressure, we use annealing to sweep through phase space as defect concentrations are reduced. We report the results of our electrical conductivity, Seebeck coefficient, and lattice size measurements as a function of composition and annealing temperature.

II. Experimental Section

Thin film samples of $CoSb_3$ were prepared using a custom-built ultrahigh vacuum deposition system, described elsewhere.[9] Samples were synthesized in a 10^{-6}−10^{-7} Torr atmosphere. Cobalt was deposited from an electron-beam gun at a rate of 0.5 Å/sec, and antimony was deposited from an effusion cell at 0.8−1 Å/sec. A computer-controlled crystal monitoring system was used to control layer thicknesses. Samples were deposited on a silicon chip, a 1-in. square piece of zero-background cut quartz, and a masked glass slide.

X-ray diffraction studies were conducted on the quartz and silicon chip using a Philips X'Pert diffractometer and a Scintag XDS-2000 θ-2θ diffractometer. X-ray reflectivity and diffraction studies were conducted on both as-deposited and annealed samples. Samples were annealed in a Thermolyne 1500 box furnace under nitrogen atmosphere, or in a tube furnace held under active vacuum. Samples were annealed for 1 h under nitrogen in a box furnace, or in a vacuum tube furnace for thirty minutes to overnight, at temperatures ranging from 200 to 600 °C. Compositional studies were conducted on a Cameca S-50 electron probe microanalysis (EPMA) instrument using 20 nA beam current, and beam voltages of 10, 15, and 20 keV.

The electrical measurements were conducted using the van der Pauw technique, with data gathered between 10 and 300 K. The mask produced a cross-shaped sample geometry that was used to minimize the effects of contact stresses during temperature cycling.[10] Four Interconnect Devices, Inc. gold-plated pogo contacts (series SS, size 40) were used, and were checked for ohmic contact before each measurement. All data were gathered under 10^{-5}−10^{-6} Torr pressure in an APD CSW-202 closed-cycle cooling system. The temperature was controlled using an Oxford ITC4, and the ambient temperature was measured with a Si diode thermometer embedded in the Cu coldfinger of the cryostat, to which the sample was attached.

The input current for the resistivity measurements was controlled using a Keithley 220 programmable current source, and measured by a Keithley 485 autoranging picoammeter. The current was input across two neighboring arms of the cross-shaped sample. The voltage was measured across the other two arms of the cross-shaped sample by a Keithley 196 DMM, and all switching was done using a Keithley 706 scanner and 7065 Hall Effect card.

The Seebeck measurements were conducted under vacuum on a line sample that had been deposited as described above. A temperature gradient of ~2 K was created using a Hewlett-Packard 6641A DC power supply. Two t-type thermocouples were used to measure the temperatures and voltages for Seebeck coefficient calculations.

III. Results and Discussion

Several samples were deposited, varying from Co-rich to Sb-rich, to test the stoichiometric range over which $CoSb_{3\pm\delta}$ could be formed, and the resulting lattice parameters. Elemental compositions were determined from electron probe microanalysis (EPMA), and the samples had ranges of compositions as intended. The samples were X-ray amorphous as deposited, and the total and layer thicknesses were calculated from the Kiessig fringes and Bragg peaks, respectively (see Figure 2). The actual thicknesses are in agreement with the intended thicknesses (see Table 2).

Thermal analysis of the $CoSb_3$ samples revealed a sharp exotherm between 140 and 180 °C. When the samples were annealed below the exotherm, no crystalline material was detectable, but when annealed at or above the exotherm temperature, all samples except A1, the most Co-rich sample (which will be omitted from further analysis), formed phase pure $CoSb_3$ (see Figure 3). This indicates that the sharp exotherm in the thermal data is due to crystallization of $CoSb_3$.

We observed a wide range of lattice constants after annealing the $CoSb_3$ samples to 200 °C, ranging from 9.026(1) Å in the most Co-rich sample, to 9.094(1) Å in the most Sb-rich sample. The range of values in these

(8) Badding, J. V.; Meng, J. F.; Polvani, D. A. *Chem. Mater.* **1998**, *10*, 2889−2894.

(9) Fister, L.; Li, X.-M.; McConnell, J.; Novet, T.; Johnson, D. C. *J. Vac. Sci. Technol., A* **1993**, *11*, 3014−3019.

(10) Elliott, G. S.; Fromko, A. D.; van de Veegaete, F.; Johnson, C. D.; Johnson, D. C. *Phys. Rev. B* **1998**, *58*, 588805−588811.

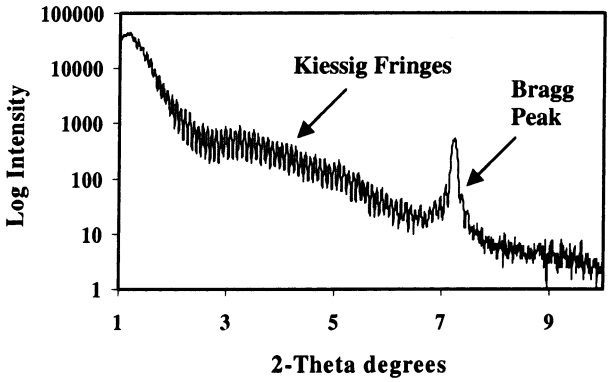

Figure 2. Low-angle X-ray diffraction data of sample A2. Large peak just above 7° 2θ is the first Bragg reflection, and small, high-frequency peaks are Kiessig fringes.

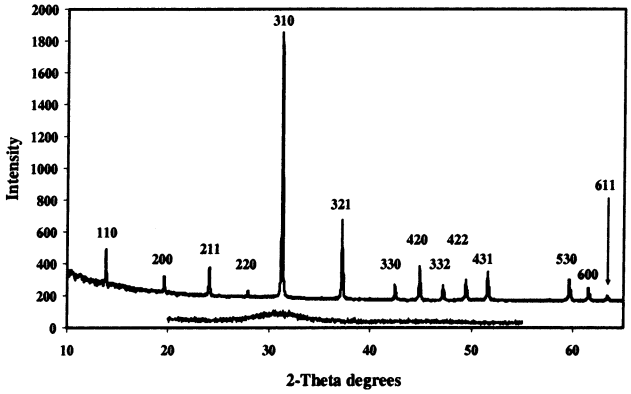

Figure 3. High-angle X-ray diffraction data: the sample is X-ray amorphous as deposited (below), and has crystallized when annealed to 200 °C (above). The Miller indices are assigned to the skutterudite peaks.

Table 2. Composition from EPMA; and Intended and Measured Layer and Total Thicknesses Calculated from Low-Angle X-ray Diffraction Data

name	% Co	% Sb	intend. layer (Å)	actual layer (Å)	intend. total (Å)	actual total (Å)
A1	31.9	68.1	11	no peaks	880	no peaks
A2	28.7	71.3	12.5	12.2	1040	1040
A3	27.4	72.6	12	11.8	1000	990
B1	25.8	74.2	14.5	13.9	1200	1180
B2	24.7	75.3	14.5	13.7	1200	1150
B3	24.4	75.6	14.5	13.6	1200	1160
C1	21.8	78.2	16.5	15.7	1360	1360
C2	18.8	81.2	18	17.5	1520	1500

lattice constants exceeds the spread found in the literature. Increased lattice sizes have previously been observed when the metal or pnictide sites are doped,[11,12] or when atoms are occupying the interstitial site.[13] An annealing study was conducted to track structural and electrical changes with annealing temperature. All samples were annealed under nitrogen in 100 °C increments from 200 to 600 °C. High-angle X-ray diffraction data were collected on each sample at each annealing temperature. Lattice parameters were calculated via Rietveld refinement for all samples and annealing temperatures.

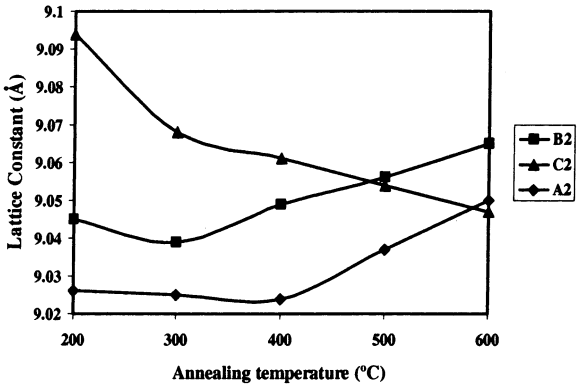

Figure 4. Trends in the lattice parameter with annealing temperature.

Three trends were observed in the lattice parameters during the annealing study on the $CoSb_3$ samples. For samples very close to the ideal 1:3 Co/Sb ratio (B1−B3), the lattice parameters decreased slightly between the 200 and 300 °C annealings, but increased during all subsequent annealings. No other crystalline phases were observed on annealing samples B1−B3. For Sb-rich samples (C1 and C2), the lattice parameters decreased consistently during each annealing step. Crystalline Sb was observed in sample C1 when annealed between 400 and 600 °C, and in C2 between 300 and 600 °C, as expected from the phase diagram.[14] For Co-rich samples (A2 and A3), the lattice parameter stayed constant through the 400 °C annealing, and then increased (see Figure 4). On annealing past 500 °C, samples A2 and A3 began to crystallize other phases, including $CoSb_2$, as expected from the phase diagram. These results suggest that when the samples crystallized at ∼150 °C, they formed over a very broad compositional range with a nonequilibrium distribution of defects.

Rietveld refinement was used to investigate the effect of the nonequilibrium defects on the structure. Sample series A and B were modeled using the typical skutterudite symmetry, $Im\bar{3}$, with 8 Co atoms and 24 Sb atoms per unit cell. As expected, these refinements fit the experimental data well, with typical R_{wp} values ranging between 0.07 and 0.10, and R_p values ranging from 0.055 to 0.09. Attempts to include Sb or Co in the interstitial positions decreased the goodness-of-fit. The observed changes in lattice constant are likely due to changes in the defect concentration, but these changes in defect concentration are too small to be modeled effectively using Rietveld refinement.

We modeled samples series C in the manner described above, but found significant differences between the observed and calculated peak intensities, particularly in the relative intensity of the (310) and (321) peaks, which are sensitive to electron density in the interstitial sites.[15] The ratio of the intensities of the (310) to the (321) peaks was significantly larger in series C (4−5) than in series A and B (2.5−3.5). Because series C was synthesized with excess Sb we included interstitial Sb

(11) Nagamoto, Y.; Tanaka, K.; Koyanagi, T. *Proc. Int. Conf. Thermoelectrics* **1997**, 16th, 330−333.
(12) Pleass, C. M.; Heyding, R. D. *Can. J. Chem.* **1962**, *40*, 590−600.
(13) Takizawa, H.; Miura, K.; Ito, M.; Suzuki, T.; Endo, T. *J. Alloys Compd.* **1999**, *282*, 79−83.
(14) Villars, P.; Calvert, L. D. *Pearson's Handbook of Crystallographic Data for Intermediate Phases*, 2nd ed.; ASM International: Materials Park, OH, 1991.
(15) Nolas, G. S.; Slack, G. A.; Morelli, D. T.; Tritt, T. M.; Ehrlich, A. C. *J. Appl. Phys.* **1996**, *79*, 4002−4008.

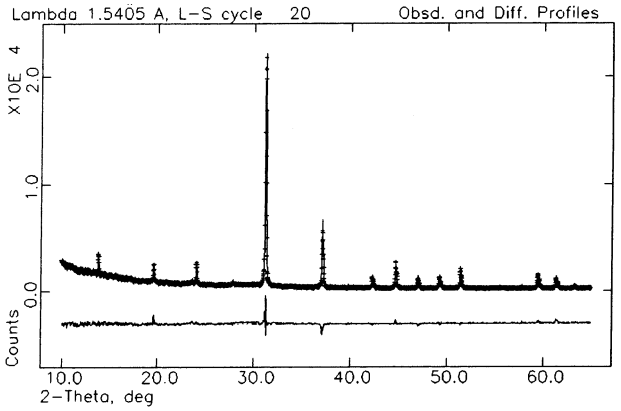

Figure 5. Rietveld refinement of sample C1, annealed for an hour at 300 °C. R_{wp} is 0.10 and R_p is 0.078. Fit was achieved with interstitial Sb at (0,0,0) and a filling fraction of 0.4. Thermal parameters for Co, Sb1, and Sb2 (interstitial) were 0.14, 0.09, and 0.8, respectively.

in the model, and this improved the fit significantly (see Figure 5). Replacing the interstitial Sb with Co vacancies worsened the fit. This provides evidence that there is Sb residing in the interstitial sites of these samples. Unfortunately, the disorder and large thermal parameters associated with the interstitial site,[16] combined with the limited *d* spacing range, make it impossible to accurately determine the fractional filling of the interstitial site using the available data.

A parallel annealing study was conducted, measuring resistivity and Seebeck coefficient at 100 °C intervals to gain further information on the changes in defect densities. The electrical resistivity and the Seebeck coefficient of narrow-band-gap semiconductors change dramatically if changes in defect populations result in changes in the carrier concentrations. In many materials, both electrons and holes contribute to the net carrier concentration, so the electrical properties that are measured reflect the combined effect of both.

In all samples, the electrical resistivity increased with annealing. From the 200 through the 300 °C annealing, the resistivity of all samples was relatively low (~1 mΩ·cm) and only slightly temperature dependent, indicating that the samples are heavily doped semiconductors (or metals). By the 400 or 500 °C annealing, the resistivity of series B and C increased 2 orders of magnitude at room temperature (~100 mΩ·cm), and showed an exponential dependence on temperature, as expected for narrow-band-gap semiconductors (see Figure 6). We calculated the approximate band gaps (see Table 3), where the slope of the linear part of the plot of $\ln(\sigma)$ vs $1/T = -E_g/2kB$.[17] These results are consistent with typical band gaps calculated for $CoSb_3$, which have ranged from 0[7] to 0.5 eV.[18] The wide range of values reported illustrates the difficulties in measuring the E_g of narrow-band-gap semiconductors. These difficulties are particularly prevalent in samples with high defect concentrations, as impurity bands can obscure the

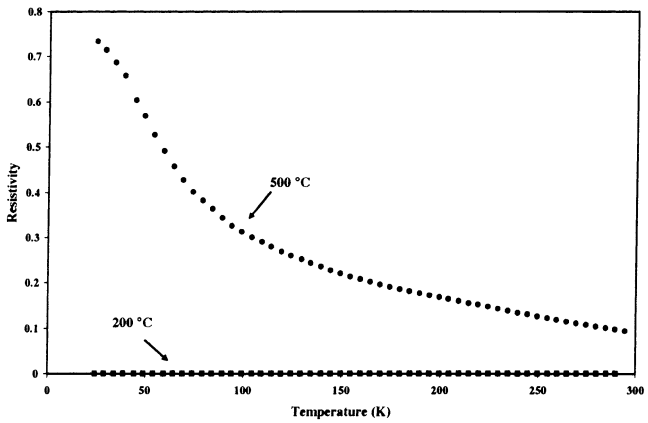

Figure 6. Electrical resistivity data at 200 and 500 °C, showing the change from low-magnitude, temperature-independent behavior to exponential behavior.

Table 3. Approximate Band Gaps for Several Samples in Series B and C

name	annealing conditions	E_g (eV)
B2	1 h @ 400 °C, N_2	0.01
B3	1 h @ 400 °C, N_2	0.01
C2	1 h @ 400 °C, N_2	0.02
C1	1 h @ 500 °C, N_2	0.08
C1	4.5 h @ 400 °C, vacuum	0.09
C1	24 h @ 400 °C, vacuum	0.10
C1	48 h @ 400 °C, vacuum	0.11

transport properties.[19] The change we observe in the resistivity reflects the decrease in carrier concentration due to decreasing defects through annealing.

Seebeck coefficients, measured as a function of temperature and annealing temperature, mirror the resistivity data, providing complimentary information about the majority carrier type. There were two main trends in the annealing dependence of the Seebeck coefficient. In sample series A, the Seebeck coefficient showed *n*-type charge carriers, and the Seebeck coefficient increased (grew more *n*-type) with increasing annealing temperatures. In a Co-rich sample we expect that the most common types of simple point defects will be interstitial Co, or Sb vacancies, either of which should produce an *n*-type sample. The increasing Seebeck coefficient as a function of annealing indicates that the number of charge carriers is decreasing, as expected for a decreasing number of defects.

For series B and C the Seebeck coefficients were relatively small (−10 to −20 μV/K), and *n*-type after the 200 and 300 °C annealing, reflecting the low-magnitude, temperature-independent resistivity observed in both series at the same annealing temperatures. The Seebeck coefficient of series C increased significantly when annealed at 400 and 500 °C, and became *p*-type. This coincided with the resisitivity of series C becoming exponential as a function of temperature, and also with the appearance of crystalline Sb in the high-angle X-ray diffraction data of series C. The exponential resistivity and increasing Seebeck coefficient indicate a decrease in carrier and defect concentrations, and the crystalline Sb indicates that interstitial Sb (detected by Rietveld refinement and intensity ratios) may be moving from the voids and into the grain boundaries. The most likely

(16) Chakoumakos, B. C.; Sales, B. C.; Mandrus, D.; Keppens, V. *Acta Chrystallogr., Sect. B* **1999**, *B55*, 341−347.
(17) Kittel, C. *Introduction to Solid State Physics*, 4th ed.; John Wiley & Sons: New York, 1971.
(18) Dudkin, L. D.; Abrikosov, N. Kh. *Zh. Neorg. Khim.* **1956**, *1*, 2096.
(19) Mandrus, D.; Migliori, A.; Darling, T. W.; Hundley, M. F.; Peterson, E. J.; Thompson, J. D. *Phys. Rev. B* **1995**, *52*, 4926−4931.

simple point defects are interstitial Sb, which should donate electrons, resulting in an *n*-type compound; and Co vacancies, which remove electron density from the sample, resulting in a *p*-type compound. The sign change in the Seebeck coefficient indicates that the defects may have originally been dominated by Sb in the voids, but annealing moved enough of it into the grain boundaries until the Co vacancies dominated the defect concentration.

Further confirmation of the changing defect concentration came with additional annealing experiments on sample C2, this time at 400 °C under active vacuum. Annealing for 24−48 h continued to increase the resistivity. The Seebeck coefficient, however, changed from *p*-type to *n*-type. The changes in majority carrier type imply that the different defects self-heal at different rates. These changes underscore the sensitivity of electrical properties to preparation and annealing conditions.

The thin-layer technique employed here allows samples to be synthesized in such a way that only limited diffusion can take place before crystallization can occur, resulting in a sample with a highly nonequilibrium defect distribution. The composition of the sample affects both the type and concentration of the defects. These starting points can be envisioned on a resistivity or Seebeck coefficient vs carrier concentration curve.[20] Annealing changes the carrier concentration, allowing us to explore a wide range of phase space with only a few samples. Each sample scans through a range of Seebeck coefficients and resistivities, producing a method that is analogous to Badding's pressure tuning of samples which allows a wide range of structural and electrical properties to manifest within a limited sample set.[8]

Acknowledgment. We gratefully acknowledge support from the National Science Foundation (DMR-9813726), the Office of Naval Research (N00014-97-1-0889), and A.S. gratefully acknowledges the support of the U.S. Department of Education Graduate Assistance in Areas of National Need Program (P200A010222).

CM030315O

(20) Mahan, G.; Sales, B.; Sharp, J. *Phys. Today* **1997**, *50*, 42−47.
(21) Sales, B. C.; Chakoumakos, B. C.; Mandrus, D. *Phys. Rev. B* **2000**, *61*, 2475